OMAERO README File

D. Stein-Zweers, M. Sneep, J.P. Veefkind, KNMI

Last update: September 5, 2011

Latest release discussed in this document: 1.2.3.1

Overview

The OMAERO Level 2 data product contains aerosol characteristics such as aerosol optical thickness (AOT), aerosol type, aerosol absorption indices as well as ancillary information. The aerosol optical thickness is retrieved from OMI spectral reflectance measurements and a best fitting aerosol type is determined. The single-scattering albedo, the layer height and the size distribution associated with the best fitting aerosol type are provided as well as diagnostic information. Each file contains the sunlit part of an OMI orbit, from the South Pole to the North Pole. In the so-called global observation mode, the OMI swath is approximately 2600 km wide, providing daily global coverage.

There are two OMI aerosol products: The OMAERUV product uses the near-UV algorithm and is described in the OMAERUV Readme File. The OMAERO product is based on the so-called multi-wavelength aerosol retrieval algorithm and is described in the present document.

The multi-wavelength algorithm is based on the spectral information in the near UV and the visible between 342.5 nm and 483.5 nm. Including the near UV wavelength range enhances the capability of the retrieval to distinguish between weakly absorbing and strongly absorbing aerosol types. Therefore, the OMAERO product can provide additional information on the aerosol type as compared to other aerosol products from sensors that do not include the near UV such as MODIS, MISR, or POLDER.

OMAERO is a standard product and has been publicly released in November 2007. OMAERO data are available at the NASA Goddard Earth Science DISC (Data and Information Services Center). For details about software versions and known problems see the OMAERO Release Specific Information. For a detailed description of the data format of the OMAERO products we refer to the Data Product Format Specification document. More information about the product can be found on the KNMI OMI website.

Apart from the orbit-based level 2 product OMAERO, OMI aerosol data from the multi-wavelength algorithm are available as geo-location based daily global level 2 G product (OMAEROG). Each OMAEROG product contains the essential aerosol data from the orbit-based OMAERO products of an entire day. This product is also available at the NASA Goddard Earth Science DISC.

Note that there is a row anomaly present in OMI data. This row anomaly affects some – but not *all* – viewing directions of OMI. This anomaly affects the quality of the Level 2 dataproducts, including OMAERO. More information can be found in the List of Known Issues and on the detailed technical information page. A careful masking of the affected rows is required before using OMAERO data. The OMAERO product contains a field that can be used for masking the row anomaly from the data.

1. Algorithm Description

The multi-wavelength algorithm uses the reflectance spectrum in the near UV and the visible wavelength range. Including the near UV enhances the capability of the retrieval to distinguish between weakly absorbing and strongly absorbing aerosol types. The main reason for this is the enhanced Rayleigh scattering in the near UV. Furthermore, mineral dust aerosol can be distinguished from weakly absorbing material by its strong absorption in the UV. Therefore, the OMAERO product can provide additional information on the aerosol type as compared to other aerosol products from sensors that do not include the near UV such as MODIS, MISR, or POLDER. The retrieval strategy of the multi-wavelength algorithm and the assumptions made are discussed briefly in this section. More information on the multi-wavelength algorithm can be found in the OMI Algorithm Theoretical Basis Document (ATBD) [RD1].

Figure 1 shows a flowchart that sketches the essential processing steps. For cloud-free scenes, aerosol parameters are derived from the sun-normalized radiance spectrum (hereafter referred to as *reflectance*) defined as

$$R(\lambda) = \frac{\pi E(\lambda)}{\cos(\theta_s) F(\lambda)} \qquad (1)$$

where $E(\lambda)$ and $F(\lambda)$ are the Earth radiance and the solar irradiance spectrum respectively and θ_s is the solar zenith angle. In the current implementation the multi-wavelength algorithm uses 14 wavelength bands, which are about 1 nm wide and are located at 342.5, 367.0, 376.5, 388.0, 399.5, 406.0, 416.0, 425.5, 436.5, 442.0, 451.5, 463.0, 477.0, and 483.5 nm. The wavelength band at 477 nm, which comprises an O_2-O_2 absorption band, is used in the OMI cloud product OMCLDO2 to derive cloud height data. This band has been included in the multi-wavelength algorithm in order to obtain more information about the aerosol height. The other bands are essentially free from molecular absorption and strong Raman signatures. A simulation study on the aerosol information content of OMI spectral reflectance measurements [RD2] shows that OMI measurements contain two to four degrees of freedom of signal. This imposes a limit on the number of aerosol parameters that can be retrieved independently and indicates that the surface reflection cannot be retrieved from OMI measured reflectance spectra independently from the aerosol parameters. The multi-wavelength algorithm accounts for these limitations using the strategies described in the following.

The multi-wavelength algorithm uses a set of aerosol models defined by size distribution, complex refractive index, and aerosol layer altitude. The models are representative for four major aerosol types including desert dust, biomass burning, volcanic and weakly absorbing aerosol. The particle shape is assumed to be spherical for all aerosol types, except for desert dust. The non-sphericity of desert dust particles is taken into account using the spheroidal shape approximation. In this approximation the irregular particles are represented by an ensemble of randomly oriented spheroidal model shapes. The single-scattering properties of the dust aerosol models have been extracted from a pre-computed light scattering database, assuming the shape distribution that is used in AERONET retrievals for non-spherical aerosol types [RD 3].

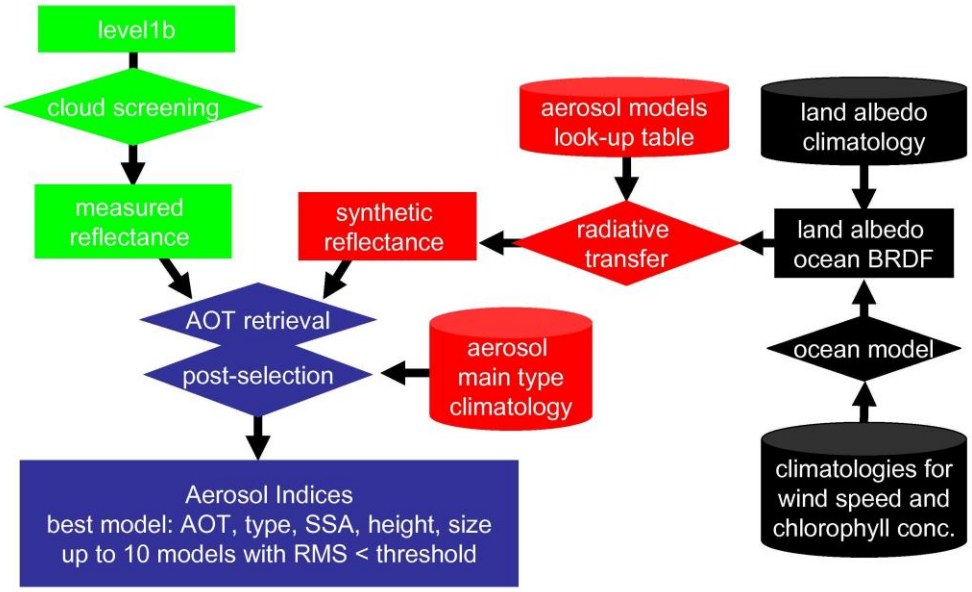

Figure 1: Flowchart of the multi-wavelength algorithm.

The choice of the aerosol models is made such that the all important aerosol types that are present in the Earth's atmosphere are represented. Note that the aerosol retrieval is constrained implicitly by this choice of the aerosol models. The on-line radiative transfer calculations are based on a pre-computed Look-Up Table (LUT) containing the radiative properties of aerosol containing atmospheres. The radiative coupling of the atmosphere with the surface is performed on-line. This approach allows efficient forward simulations for scenes with a given aerosol model, AOT, viewing geometry and given surface reflection properties. The surface reflection is taken from an ocean model or a land albedo climatology (see Section 1.1).

The aerosol parameters are determined by evaluating the merit function Ψ_m

$$\Psi_m = \sum_{l=1}^{L} \left(\frac{R^*(\lambda_l) - R_m(\tau(\lambda_{ref}), \lambda_l)}{\varepsilon(\lambda_l)} \right)^2 \quad (2)$$

where $R^*(\lambda_l)$ is the measured reflectance, $R_m(\tau(\lambda_{ref}), \lambda_l)$ is the reflectance for the aerosol model m as a function of the aerosol optical thickness at the reference wavelength $\tau(\lambda_{ref})$, and $\varepsilon(\lambda_i)$ is the error in the measured reflectance. The optimal aerosol optical thickness is determined for each aerosol model by a non-linear fitting routine using a modified Levenberg-Marquardt method [RD4]. The choice of the aerosol models made by the retrieval is constrained in a post-selection that uses an aerosol main type climatology. The aerosol main type climatology has been derived from a chemical transport model (TM5) for the year 2005. In this way only aerosol types are allowed that can be expected for a given geo-location and time of the year. Note that the aerosol climatology can allow for more than one aerosol main type for a given scene. Amongst the post-selected aerosol models the aerosol model with the smallest Ψ_m is selected for the present ground pixel. The SSA, the size distribution and the aerosol height are directly determined by the selected aerosol model. A cloud screening scheme is applied in order to exclude cloudy scenes from the retrieval; ocean scenes that are affected by specular reflection at the sea surface (sun-glint) are flagged such that they can be excluded from the analysis of the retrieved data (see Section 1.2).

The level 2 product also contains information on the quality of the retrieved aerosol parameters. The precision in the retrieved AOT is given in terms of the retrieval error of the non-linear fitting routine. The AOT, SSA and Root Mean Square (RMS) of the residual reflectance of up to ten aerosol models with an RMS lower than a given threshold value are included in order to provide information about how well the best selected aerosol model is defined.

1.1 Surface reflection

The surface reflection cannot be retrieved from OMI measured reflectance spectra independently from the aerosol parameters. Over oceans the spectral bidirectional reflectance distribution function (BRDF) of the surface is computed using a model that accounts for the chlorophyll concentration of the ocean water and the near-surface wind speed [RD5]. The chlorophyll concentration is taken from a climatology that has been derived from monthly averaged data from the MODIS ocean color product. Over land the surface albedo spectrum is taken from a global seasonally resolved climatology assuming Lambertian reflectance at the surface. This surface albedo climatology has been generated from 5 years worth OMI data [RD6]. The relatively small pixel size of OMI yields a probability of observing cloud free scenes that is sufficiently high in order to extract surface reflection properties from OMI reflectance spectra.

1.2 Cloud and Sun-glint screening

Three tests are applied in order to exclude cloudy scenes from the retrieval. The first test excludes bright scenes with very low absorption using reflectance data in combination with the UV aerosol index. Scenes with a reflectance larger than the threshold value of

0.3 and a UV aerosol index below 0.12 (low absorption) are classified as cloudy. The second test uses cloud fraction data from the OMI O_2-O_2 cloud product (OMCLDO2). Scenes with a cloud fraction larger than 0.34 are classified as cloudy. The third test is based on the spatial homogeneity of the scene. OMI level 1b radiance data are spatially binned. OMI level 1b radiance data contain the small pixel variance, which is a measure for the spatial homogeneity of the scene within one pixel. Inhomogeneous scenes with a small pixel variance larger than 0.00015 times the average radiance value (standard deviation larger than ~1 % of the average radiance value) are classified as cloudy. Note that the spatial homogeneity test is capable of screening out a large part of the cloudy scenes. A large cloud fraction threshold is hence chosen in order to avoid screening out of desert dust scenes to which the O_2-O_2 cloud product tends to assign large cloud fraction values. Note that unrecognized cloud contamination leads to an overestimation of the AOT and is considered to be one of the most important error sources.

Ocean scenes that are affected by specular reflection at the sea surface (sun-glint) should be excluded from analyses of the retrieved aerosol data. Sun-glint screening can be performed using the sun-glint warning flag (bit 4 of the ground pixel quality flag) provided in the OMAERO product. The sun-glint warning flag is raised when the sun-glint angle (emergent zenith angle relative to the specular reflection angle [RD9]) is smaller than 40 degrees.

2 Data Quality Assessment

Various validation studies have been made for the aerosol optical thickness from the OMAERO product using ground based, airborne, and satellite based observations. The largest issues are with cloud contamination. A significant number of OMAERO pixels subpixel cloudiness that leads to errors in the aerosol parameters. Therefore it is best to use external cloud clearing information with OMAERO data.

For ocean scenes, global AOT data from the OMAERO product have been compared with measurements from other satellite instruments. Here we show such a comparison for the period of June 2006.

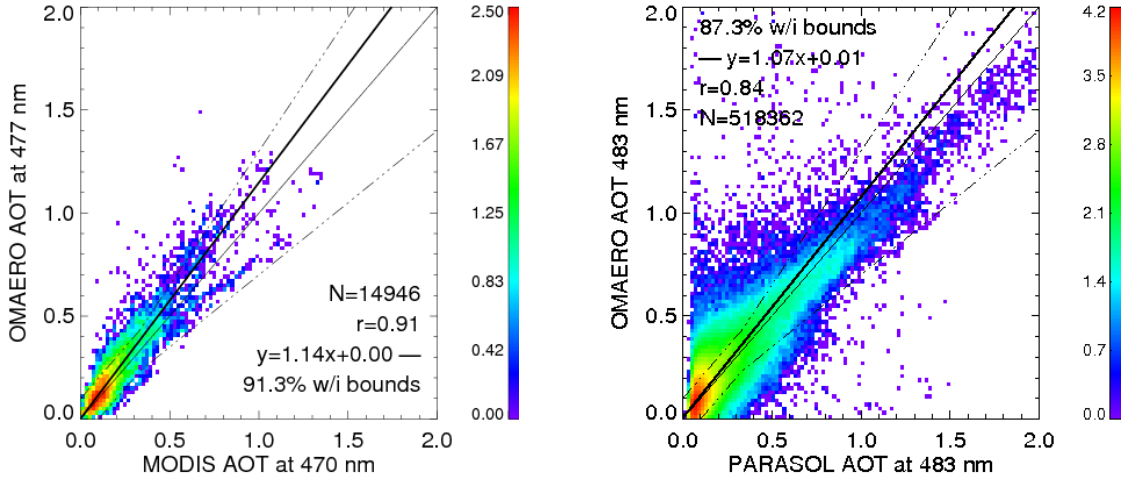

Figure 2: AOT from the OMAERO product compared with quality assured data from the MODIS standard product (left) and with quality parameter filtered data from POLDER (right).

The comparison with quality assured data from the MODIS standard product (Fig.2, left) shows excellent agreement between the datasets. For this comparison only quality assured MODIS data (QA flag=3) have been included. By using this data flag many partly clouded OMI scenes are excluded that are not recognized as being cloudy by the OMI cloud screening scheme. When OMI data are used alone, unrecognized cloud contamination is an important source of errors. For the comparison with POLDER on the PARASOL platform, the data have been filtered based on the quality parameter given by the POLDER aerosol algorithm. A correlation coefficient of larger than 0.8 and a slope of the regression line of 1.07 indicate a good agreement between the datasets.

For land scenes, we report the results of various validation studies. Curier et al. (2007) [RD8] have investigated the AOT data from the OMAERO product for Europe and adjacent oceans. A comparison with MODIS AOT data yields correlation coefficients between 0.76 and 0.81 for ocean and between 0.59 and 0.70 for land. The difference between land and sea is due to shortcomings in the currently used surface albedo climatology. In the same study strongly site-dependent correlations are reported for comparisons of the AOT from the OMAERO product with ground based data from various AERONET stations in Europe.

The level 2 product contains diagnostic information about the quality of the fit. Typical values for the retrieval error of the AOT obtained using the non-linear fitting routine are below 0.03. This error concerns the AOT retrieval for a given aerosol model and hence does not include error correlations of AOT and microphysical aerosol parameters or the aerosol height. The standard deviation of the AOT values of the aerosol models with an RMS lower than a given threshold is below 0.11 for 95% of the cases. The standard deviation of the SSA values of the aerosol models with an RMS lower than a given threshold is below 0.1 in 95% of the cases.

3 Product Description

A single OMAERO product file contains all OMI measurements on the sunlit portion of the Earth, for one Aura orbit. During one orbit OMI performs approximately 1650 measurements, which take 2 seconds each. In the global observation mode, 60 across track ground pixels are measured simultaneously during a measurement. These 60 measurements cover a swath of approximately 2600 km wide. During so-called zoom-in measurements the swath width is reduced. The operational baseline includes zoom-in measurements for 1 day a month. In case of zoom-in measurements 30 of the 60 across track pixels contain data, the other 30 contain fill values.

Aerosol characteristics such as aerosol indices, the aerosol optical thickness and the aerosol model that has been selected as the best fitting model by the multi-wavelength algorithm, are provided in the product file for each ground pixel. The aerosol optical thickness and the single-scattering albedo of the best fitting model is given for all wavelengths used in the retrieval. Additionally, the aerosol optical thickness and the single-scattering albedo of models with a merit function below a given threshold are provided for the diagnostic wavelengths 342.5, 367.0, 388.0, 406.0, 425.5, 442.0, 463.0, 477.0, and 483.5 nm (see attribute data fields in the product file). The standard deviation of the AOT and SSA values of the models that passed the threshold, given in the level 2 product, is a measure for how well the best fitting model is defined by the retrieval. An error-weighted average of AOT and SSA of the models that passed the threshold can be used alternatively to the AOT of the best fitting model.

The across-track quality flag (field "XTrackQualityFlags") indicates whether a row is affected by the row anomaly. Bit 0 of this flag indicates that the Level-1b data from the UV2 channel are classified as affected. Bit 1 of this flag indicates that the Level-1b data from the Vis channel are classified as affected. It is strongly recommended to consult the DISC website (see http://disc.gsfc.nasa.gov/Aura/OMI/) and the detailed technical information page in order to obtain the most recent status of the row anomaly and the related quality flagging.

A complete description of the format of the OMAERO data product is available in the Product Format Specification.

The OMAERO product is written as an HDF-EOS5 swath file. For a list of tools that read HDF-EOS5 data files, please visit this link: http://disc.gsfc.nasa.gov/Aura/tools.shtml. The OMI level 2 products can be read using an IDL reading routine that can be found at the KNMI product site.

4 Data Availability

The OMAERO product is available through the NASA Goddard Earth Science DISC. Subsets of these data over many ground stations and along Aura validation aircraft flights paths will also be made available through the Aura Validation Data Center (AVDC) website) to those

investigators who are associated with the various Aura science teams. Christian Retscher is the point of contact at the AVDC.

5 Contact Information

Questions related to the OMAERO dataset should be directed to gsfc-help-disc@lists.nasa.gov. For questions and comments related to the OMAERO algorithm and data quality please send a mail to omaero@ltpmail.gsfc.nasa.gov.

OMAERO Release Specific Information

Maarten Sneep, Pepijn Veefkind
September 5, 2011

Known Issues List

The following contains a list of known issues in the OMAERO data product:

1. There is a “row anomaly” present in OMI data, affecting some (but not all) viewing directions of OMI. Details on the starting dates of the various stages of the development of this anomaly can be found on the web. The row anomalies have four distinct effects on the OMI radiance spectra:
   (1) A decrease in the radiance level for several viewing directions. It is currently assumed that this is caused by a partial blocking of the OMI nadir port. The blocking object is assumed to be opaque. This is effectively a multiplicative error on the radiances.
   (2) An increase in the radiance level at (mostly) the same viewing directions as are affected by a decrease in the radiance for the northern part of the orbit. This occurs when the part of OMI containing the nadir port is directly illuminated by the sun. This is assumed to be caused by reflection of sunlight into the nadir port via the blocking object (outside of OMI). This is an additive error on the radiances.

   This increase in the radiance level is not observed for the first anomaly in rows 53-54 (0-based).
   (3) The blocking object causes an inhomogeneous illumination of the spectral slit in OMI. This causes a change in the slit function, shifting the center of weight away from the nominal center. This causes light of a specific wavelength to hit the detector in a slightly different location than expected.

   In the OMI level 0 to level 1 software, the wavelengths are not fitted, but assigned. Corrections are made based on the homogeneity of clouds and the temperature of the optical bench. Therefore the effect of an object blocking part of the incoming light is not included in the nominal level 1B wavelength assignment.
   (4) Light reflected by the earth from outside the nominal field of view is coupled into the nadir port. This light is collected over a large area, giving an additive error on the radiances, with a not quite constant term.

   ←

   The XtrackQualityFlags field present in OMAERO version 1.2 and later indicates which rows are affected by the row anomaly. A non-zero value in the XTrackQualityFlags indicates that the pixel is affected by the row anomaly. Please be aware that for all other rows the data are of optimal quality and not affected. Also all OMI data before these anomalies are of optimal quality.

2. The cloud screening scheme does not detect all cloud contaminated pixels. The retrieved aerosol parameters at some pixels may therefore be affected by the presence of clouds.
3. In some cases the multi-wavelength algorithm tends to select aerosol models with too large absorption.
4. The radiometric calibration shows inconsistencies in the across-track direction causing along-track stripes in the aerosol indices provided by the OMAERO product.

Release History

OMAERO v1.2.3.1

This is an incremental update to version 1.2 of the OMAERO product, September 2011. Some changes were made to the handling of snow or ice at the surface within a library shared with OMCLDO2, OMDOAO3 and OMNO2. Since these pixels were not processed by OMAERO the effect for OMAERO is minimal.
This version is used to reprocess the OMAERO for the complete mission. The L1B used for reprocessing has been post-processed to include updated information on the row anomaly. This OMAERO dataset will therefore include up to date information on the row anomaly for the whole mission.

OMAERO v1.2:

Changes introduced in version 1.2 of the OMAERO product, November 2010.

1. Added orbit phase field that is copied from L1B.
2. Updated XTrackQualityFlags handling, combining information from both the UV2 and VIS channels.
3. Added propagation of XTrackQualityFlags into error flags controlled by OPF XTrackQualityFlagsErrorMask parameter. In this release no anomaly errors are propagated into the normal error flags, this may change in a future release.
4. The OMI L1B contain two wavelength calibration methods, a full fit and an assignment based on temperature and cloudiness. For OMAERO the wavelength assignment is not critical, and assigned wavelengths are used for the whole mission.
5. Corrected some dimension sizes in SmallPixelWavelengthUV and SmallPixelWavelengthVIS fields.
6. An update to the surface albedo database is used, using five years of OMI data. This database is an update to the database published in the Journal of Geophysical Research (Q.L. Kleipool, M.R. Dobber, J.F. de Haan and P.F. Levelt, *Earth surface reflectance climatology from 3 years of OMI data*, J. Geophys. Res., 2008, **113**, doi:10.1029/2008JD010290). The database is available for download, including information on the changes.
7. A configuration error caused OMAERO to use the daily OMI irradiance, rather than a yearly average of the irradiance. This has been corrected.

OMAERO v1.1.1:

1. updated version v 1.1.1 land surface albedo climatology based on 3 years of OMI data, The across-track quality flags introduced in the Level 1B data from the UV2
2. Public release v 1.0.6. November 2007
3. Provisional release in December 2006.

Related Documents

[RD1] Torres, O., R. Decae, J.P. Veefkind, and G. de Leeuw (2002): OMI Aerosol Retrieval Algorithm, in OMI Algorithm Theoretical Basis Document: Clouds, Aerosols, and Surface UV Irradiance, Vol. 3, version 2, (OMI-ATBD-03, P. Stammes, Ed.), http://eospso.gsfc.nasa.gov/eos_homepage/for_scientists/atbd/docs/OMI/ATBD-OMI-03.pdf.

[RD2] Veihelmann, B., P.F. Levelt, P. Stammes and J.P. Veefkind (2007): Aerosol Information Content in OMI Spectral Reflectance Measurements, Atmos. Chem. Phys., 7, 3115-3127.

[RD3] Dubovik, O., et al. (2006): Application of spheroid models to account for aerosol particle nonsphericity in remote sensing of desert dust, J. Geophys. Res., 111, D11208, doi:10.1029/2005JD006619.

[RD4] More, J.J. (1978): The Levenberg-Marquardt algorithm: implementation and theory. In Numerical Analysis Proceedings (Dundee, June 28 - July 1, 1977, G. A.Watson, Editor), Lecture Notes in Mathematics 630, Springer-Verlag.

[RD5] Veefkind J.P. and G. de Leeuw (1997): A new aerosol retrieval algorithm applied to ATSR-2 data Journal of Aerosol Science, Volume 28, Supplement 1, pp. 693-694(2).

[RD6] Kleipool, Q. L.; Dobber, M. R.; de Haan, J. F.; Levelt, P. F. (2008): Earth surface reflectance climatology from 3 years of OMI data, J. Geophys. Res., Vol. 113 (D18), DOI: 10.1029/2008JD010290. The dataset itself is available from the OMI website.

[RD7] Herman, J.R., and E. Celarier (1997): Earth surface reflectivity climatology at 340 and 380 nm from TOMS data, J. Geophys. Res., Vol. 102, 12,059-12,076.

[RD8] Curier R.L., J.P. Veefkind, R. Braak, O.Torres, G. de Leeuw (2007): Retrieval of aerosols optical properties from OMI radiances using a multi-wavelength algorithm: Application and validation to Western Europe, J. Geophys. Res., in press.

[RD9] King, M.D., Y.J. Kaufman, D. Tanre, and T. Nakajima (1999): Remote Sensing of Tropospheric aerosols from Space: Past, present and future, Bull. Am. Meteorol. Soc,. 80, 2229-2259.